Energy-Efficient Resource Allocation for Dual-NOMA-UAV Assisted Internet of Things

Zechen Liu, Xin Liu, *Senior Member, IEEE,* Victor C. M. Leung, *Life Fellow, IEEE,* and Tariq S Durrani, *Life Fellow, IEEE*

***Abstract*—Employing unmanned aerial vehicles (UAVs) characterized by low cost, high maneuverability, and on-demand deployment as aerial base stations (BSs) of Internet of Things (IoT) can guarantee communication performance in the absence of terrestrial BSs. However, the limited energy budget of UAV constrains its development. In this paper, a dual-UAV-assisted IoT using non-orthogonal multiple access (NOMA) is proposed to improve IoT capacity. To reduce energy consumption of the UAVs while ensuring a certain throughput, a joint resource optimization problem of communication scheduling, transmit power and motion parameters of UAVs is formulated to maximize energy efficiency of UAVs. To solve the proposed non-convex optimization problem, we present an alternating iterative optimization algorithm to alternately optimize three sub-problems: communication scheduling optimization, UAV transmit power optimization and UAV motion parameters optimization, each of which can be converted into convex optimization and solved using Lagrange multiplier method, subgradient descent method and successive convex approximation (SCA). The numerical results show that optimizing UAV motion parameters can effectively improve energy efficiency of UAVs, and the proposed dual-NOMA-UAV assisted IoT can achieve higher energy efficiency than the orthogonal multiple access (OMA)-UAV assisted IoT.**

***Index Terms*—IoT, UAV, NOMA, resource allocation, energy efficiency maximization.**

I. Introduction

As an important information network integrating the real world and the digital world, Internet of Things (IoT) has played an important role in medical care, transportation, etc [1]-[3]. At present, IoT devices mainly rely on terrestrial base stations (BSs) for information transmissions. However, due to the extensive application scenarios of IoT, IoT devices do not work well when deployed in the target areas lacking BS's coverage [4]-[6]. Under this circumstance, unmanned aerial vehicle (UAV) with the advantages of low cost, high mobility and on-demand deployment is used as aerial BS to assist IoT. Compared with the terrestrial BS, the channels between UAVs and IoT devices are often line-of-sight (LoS), resulting in better communication quality for UAV assisted IoT [7]-[11].

There have been several researches on UAV-assisted IoT. In [12], Gu *et al.* designed a rotary-wing UAV enabled IoT, where the completion time was minimized by jointly optimizing transmit power and trajectory of UAV under energy-limited constraint. In [13], a multi-UAV assisted wireless power communication network was proposed by Wang *et al.*, where the minimum communication rate of all the users was maximized by synergistically optimizing communication scheduling, user transmit power, UAV trajectory and subplot duration. In [14], Li *et al.* minimized data loss of UAV-aided IoT using deep reinforcement learning to optimize UAV flight cruise control and data collection schedule. In [15], an unsupervised trajectory optimization was proposed by Zhu *et al.*, where a sequential deep reinforcement learning model was used to minimize system energy consumption. In [16], Yang *et al.* proposed UAV-aided edge computing for IoT, where the UAVs with limited local computing capabilities acted as mobile-edge computing devices to serve the terrestrial IoT nodes. By differential evolution based multi-UAV deployment, the UAVs achieved load balance while satisfying both quality of service (QoS) of IoT nodes and coverage constraint. In [17], a UAV-assisted wireless communication system was put forward by Zeng *et al.*, where UAV is deployed to communicate with ground nodes. The total energy consumption was minimized by optimizing communication time and trajectory of UAV. In [18], Wu *et al.* maximized minimum throughput of all devices by optimizing UAV trajectory and resource allocation under the constraint of communication delay. In [19], a multi-UAV assisted cooperative secure network was proposed by Hua *et al.*, where the secrecy energy efficiency was maximized by jointly optimizing communication power, communication scheduling and trajectory of UAV. In [20], Zeng *et al.* proposed a propulsion energy consumption model for fixed-wing UAV, where energy efficiency of UAV with unconstrained and generally constrained trajectories was maximized by successive convex approximation (SCA), respectively. In [21], a multi-UAV assisted wireless communication network was proposed by Wu *et al.*, where the minimum throughput was maximized by jointly optimizing trajectory, transmit power and user scheduling of UAV via block coordinate descent and SCA method. In [22], Li *et al.* proposed a static UAV relays assisted Space-Air-Ground Internet of remote things network, where the energy efficiency was maximized by jointly optimizing the selection of sub-channel, the power control of uplink transmission and the deployment of static UAV relays.

This work was supported in part by the Guangdong "Pearl River Talent Recruitment Program" under Grant 2019ZT08X603, in part by the Guangdong "Pearl River Talent Plan" under Grant 2019JC01X235, and in part by the Fundamental Research Funds for the Central Universities under Grant DUT21JC20. (*Correspondence author: Xin Liu*)

Z. C. Liu and X. Liu are with the School of Information and Communication Engineering, Dalian University of Technology, Dalian 116024, China (e-mail: lzc_sdzb@mail.dlut.edu.cn; liuxinstar1984@dlut.edu.cn).

Victor C. M. Leung is with the College of Computer Science and Software Engineering, Shenzhen University, Shenzhen, China 518060 (e-mail: vleung@ieee.org).

T. S. Durrani is with the Department of Electronic and Electrical Engineering, University of Strathclyde, Glasgow G1 1XQ, U.K. (e-mail: t.durrani@strath.ac.uk).

This is a peer reviewed, accepted author manuscript of the following research article: Liu, Z., Liu, X., Leung, V. C. M., & Durrani, T. S. (2022). Energy-efficient resource allocation for dual-NOMA-UAV assisted Internet of Things. IEEE Transactions on Vehicular Technology, 1-13. https://doi.org/10.1109/tvt.2022.3219236

The above literatures mainly focus on UAV-assisted IoT based on orthogonal multiple access (OMA). However, as the number of IoT devices continues to increase, spectrum resources are becoming increasingly scarce. Under this circumstance, non-orthogonal multiple access (NOMA) technology is applied to improve spectrum utilization and user capacity. Some literatures have considered NOMA for UAV assisted communications. In [23], Katwe *et al.* proposed a UAV-assisted full-duplex NOMA cellular network, whose throughput was maximized by dynamically user clustering and jointly optimizing transmit power and placement of UAV. In [24], Wang *et al.* proposed a graph-based file dispatching protocol to effectively minimize the time for UAV auxiliary tasks in a NOMA-UAV network. In [25], Wu *et al.* used K-means clustering algorithm to group nodes and maximized the minimum system rate by optimizing scheduling and trajectory of UAVs. In [26], Hu *et al.* maximized achievable rate of a specific user served by UAV via jointly optimizing decoding order, transmit power and placement of UAV. In [27], Do *et al.* proposed a full-duplex UAV relay assisted information transmission NOMA network, where the distant users can jointly communicate to two nearby base stations. The authors considered the imperfect successive interference cancellation at each receiver and used outage probability as one of the performance metrics.

The aforementioned researches on NOMA-UAV ignore the issue of UAV energy consumption, which is great important for UAVs with limited energy. To make the energy-constrained UAVs work more efficiently, some literatures have considered energy efficiency of UAV in NOMA-UAV system. In [28], a time sharing NOMA-UAV assisted communication system was proposed by Masaracchia *et al.*, and the maximum energy efficiency of UAV was achieved by a dual-layer iterative algorithm. In [29], under the constraints of UAV placement and power budget, Katwe *et al.* maximized energy efficiency of UAV assisted full-dulplex NOMA system by jointly using Dinkelbach method, SCA method and particle swarm optimization. In [30], Sohail *et al.* proposed a NOMA-UAV communication scheme to satisfy high traffic requirement of wireless network. Considering communication and hovering consumption of UAV, the authors maximized energy efficiency of UAV by the Dinkelbach algorithm under different grouping methods. In [31], Zhang *et al.* maximized energy efficiency of multi-UAV system by optimizing user scheduling and communication power with a probability constraint for imperfect channel state information (CSI).

However, the above researches only consider a static UAV and ignore the UAV movement in energy efficiency optimization. Some literatures have optimized UAV trajectory to improve energy efficiency. In [32], Li *et al.* optimized trajectory and resource allocation of UAV to maximize total system energy efficiency. However, the authors only assumed a fixed propulsion power for the UAV and made a simple distance constraint on the UAV trajectory without considering the kinematic constraints. In fact, the propulsion power and trajectory of UAV are often varied with the UAV flight. In [33], Liu *et al.* proposed a multi-UAV enabled NOMA IoT, where multiple UAVs in the target area are deployed to provide services for IoT nodes with different rate requirements by a circle packing scheme. And fair energy efficiency among UAVs was achieved by jointly optimizing communication resources and trajectories of UAVs. However, the authors assumed the flying speeds of UAVs to be constant without considering varied UAV speeds and kinematic constraints.

In this paper, a dual-NOMA-UAV enabled IoT is proposed, where the UAVs are dispatched as aerial BSs to serve terrestrial IoT devices. The energy efficiency of UAVs is maximized by considering both varied UAV speeds and kinematic constraints. The contributions of this paper are summarized as follow.

- A dual-NOMA-UAV assisted IoT model is established, where two UAVs fly over the corresponding regions and serve the terrestrial IoT nodes. We propose a NOMA grouping algorithm to pair the IoT nodes in different regions for achieving great distance differences.
- We formulate an efficient optimization problem to maximize energy efficiency of mobile UAVs by jointly optimizing user scheduling, transmit power and motion parameters of UAVs. Specifically, we consider the changed propulsion power consumption of UAVs under varied UAV speeds, which accords with the actual flight situations of UAVs.
- The non-convex optimization problem is separated into three sub-problems: communication scheduling optimization, UAV transmit power optimization and UAV motion parameters optimization. By jointly using Lagrange multiplier method, sub-gradient descent method and SCA method, we can deal with the initial optimization problem by proposing an alternating iterative optimization algorithm.

The rest of this paper is organized as follows. In Section II, we describe a dual-NOMA-UAV assisted IoT model, and formulate a resource optimization problem. In Section III, the initial non-convex optimization problem is divided into three sub-problems to be solved separately, and an alternating iterative optimization algorithm is proposed to get the optimal solution. In Section IV, some numerical simulation results are presented and analyzed. Finally, we conclude the paper in Section V.

II. System Model And Problem Formulation

A. System Model

Consider a dual-UAV assisted NOMA IoT in Fig. 1. We suppose K IoT nodes are randomly and uniformly distributed in a circular area of radius r_{out} and served by two UAVs, and the UAVs periodically fly over the corresponding regions for performing NOMA transmissions. In the NOMA, the UAV transmits signals to the IoT nodes with different power through superposition coding, and each node demodulates the received signal through successive interference cancellation (SIC). The transmit power levels for different nodes are determined by the distance from UAV to each node. The node far away from the UAV will be allocated more transmit power to guarantee the required communication rate, while the node close to the UAV can eliminate the interference of high-power signal through SIC. Therefore, the NOMA performance can be improved via

pairing a near node and a far node into a group. We divide the target area into inner circle of radius r_{in} and annular region of radius $r_{out} - r_{in}$. Assuming that the nodes are uniformly distributed in the target area, we set $r_{in} = \frac{r_{out}}{\sqrt{2}}$ to guarantee that there are the same number of nodes in the inner circle and annular region. Then, we pair the nodes in the inner circle with those in the annular region to form $I = K/2$ NOMA groups with great distance differences.

A 3D Cartesian coordinate system has been established to denote the range of each region and the location of each node. We suppose that two UAVs fly over inner circle and annular region with a fixed altitude H, respectively. We divide UAV flight time T into N time slots, and the length of each time slot δ_t is small to ensure that the UAV state is constant in each time slot. We denote the node coordinates as $q_{i,j} = (x_{i,j}, y_{i,j}, 0)$ for $j = 1, 2$ and $i = 1, 2, ..., I$, where $j = 1$ and $j = 2$ denote the nodes locating in annular region and inner circle region, respectively. Similarly, the real-time coordinate of the UAVs can be described as $q_m(t) = (x_m(t), y_m(t), H)$ for $t = 1, 2, ..., N$ and $m = 1, 2$, where $m = 1$ and $m = 2$ represent the UAVs flying over annular region and inner circle region, respectively. In order to guarantee that the UAVs fly over the designated regions, the flight range constraints of the UAVs can be given as

$$r_{in} < d_{m,z}(t) \leq r_{out}, m = 1 \tag{1}$$

$$0 < d_{m,z}(t) \leq r_{in}, m = 2 \tag{2}$$

where $d_{m,z}(t)$ denotes the distance from UAV m to axis z at time slot t. Based on the flight area limitations, the two UAVs have their own near and far nodes, respectively, which can better utilize the advantages of NOMA grouping.

Since the UAVs perform fixed circular flight, the initial and end positions of each UAV should be the same. Moreover, the UAV trajectory should satisfy the kinematic constraints and safety distance constraints, which can be described as

$$q_m(1) = q_m(N), \forall m \tag{3}$$

$$q_m(t+1) = q_m(t) + V_m(t)\delta_t + \frac{1}{2}a_m(t)\delta_t^2, \forall m, t \tag{4}$$

$$V_m(t+1) = V_m(t) + a_m(t)\delta_t, \forall m, t \tag{5}$$

$$||q_1(t) - q_2(t)||^2 \geq d_{\min}^2, \forall t \tag{6}$$

where $d_{\min}$ denotes the minimum distance between UAVs to prevent collisions, $V_m(t)$ and $a_m(t)$ denote the flying speed and acceleration of UAV m at time slot t, respectively.

We assume that the channels between nodes and UAVs can be regarded as LoS channel, where the Doppler effect caused by UAV movement can be effectively compensated [20]. Therefore, the channel power gain from the UAV m to the node j of the group i can be given as

$$h_{m,i,j}(t) = \frac{\beta_0}{d_{m,i,j}^2(t)} = \frac{\beta_0}{||q_m(t) - q_{i,j}||^2} \tag{7}$$

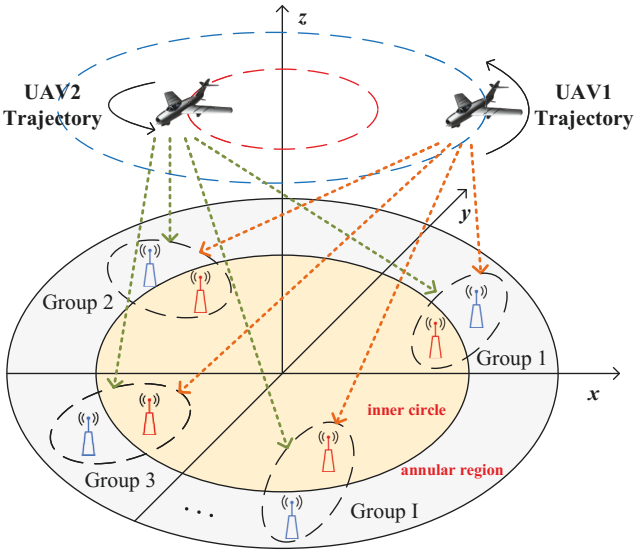

Fig. 1: System model.

where β_0 indicates the channel power gain at the reference distance $d_0 = 1$m, and $d_{m,i,j}(t)$ denotes the distance from the UAV m to the node j of the group i.

We introduce a binary variable $u_{m,i}(t)$ to indicate the communication scheduling of UAV. If UAV m serves NOMA group i at time slot t, $u_{m,i}(t) = 1$, otherwise, $u_{m,i}(t) = 0$. Furthermore, we assume that each group can only be connected to one UAV while each UAV can only provide service for one group in each time slot. The constraints for $u_{m,i}(t)$ can be given as

$$u_{m,i}(t) = \{0, 1\}, \forall m, i, t \tag{8}$$

$$\sum_{i=1}^{I} u_{m,i}(t) \leq 1, \forall m, t \tag{9}$$

$$\sum_{m=1}^{2} u_{m,i}(t) \leq 1, \forall i, t \tag{10}$$

In a NOMA group, the node farther from the UAV will be allocated more transmit power to satisfy the minimum communication rate, i.e., $P_{m,i,1} < P_{m,i,2}$ at $m = 1$ and $P_{m,i,1} > P_{m,i,2}$ at $m = 2$, where $P_{m,i,j}(t)$ represents the transmit power from UAV m to the node j of the group i.

The two nodes in one group can share the same spectrum resources by multiplexing their transmit power at the UAVs. Using SIC for NOMA decoding, the high-power node is first decoded, and then the low-power node is decoded by removing the high-power signal from the received signal. Hence, the communication rate of the group i served by UAV m can be given as

$$R_{m,i}(t) = \log_2\left(1 + \frac{P_{m,i,1}(t)\, h_{m,i,1}(t)}{\sigma^2}\right) + \log_2\left(1 + \frac{P_{m,i,2}(t)\, h_{m,i,2}(t)}{\sigma^2 + P_{m,i,1}(t) h_{m,i,2}(t)}\right), \forall i, m = 1 \tag{11}$$

$$R_{m,i}(t) = \log_2\left(1 + \frac{P_{m,i,1}(t)\, h_{m,i,1}(t)}{\sigma^2 + P_{m,i,2}(t) h_{m,i,1}(t)}\right) + \log_2\left(1 + \frac{P_{m,i,2}(t)\, h_{m,i,2}(t)}{\sigma^2}\right), \forall i, m = 2 \quad (12)$$

where σ^2 represents the noise power.

Furthermore, throughput of the UAV m and total system throughput in a flight cycle time T can be respectively given as

$$R_m = \sum_{t=1}^{N} \sum_{i=1}^{I} u_{m,i}(t) R_{m,i}(t), \forall m \quad (13)$$

$$R_{total} = R_1 + R_2 \quad (14)$$

For fixed-wing UAVs, the total consumed power includes transmit power and propulsion power. From [20], the propulsion power of UAV m can be given as

$$P_m^c(t) = c_1 \parallel V_m(t) \parallel^3 + \frac{c_2}{\parallel V_m(t) \parallel}(1 + \frac{\parallel a_m(t) \parallel^2}{g^2}) \quad (15)$$

where $a_m(t)$ is the acceleration of UAV m, g is the gravitational acceleration, the constants c_1 and c_2 are related to air density and UAV hardware conditions.

Accordingly, the power consumption of UAV m and total system power consumption in a flight cycle time T can be given as

$$E_m = \sum_{t=1}^{N} \left(P_m^c(t) + \sum_{i=1}^{I} u_{m,i}(t) P_{m,i}(t) \right) \quad (16)$$

$$E_{total} = E_1 + E_2 \quad (17)$$

where $P_{m,i}(t) = P_{m,i,1}(t) + P_{m,i,2}(t)$ denotes the total transmit power of UAV m serving group i at time slot t.

B. Problem Formulation

To improve the throughput while reducing the energy consumption, we seek to maximize energy efficiency by jointly optimizing communication scheduling $\mathbf{U} = \{u_{m,i}(t), \forall m, i, t\}$, UAV transmit power $\mathbf{P} = \{P_{m,i}(t), \forall m, i, t\}$ and UAV motion parameters $\mathbf{G} = \{q_m(t), a_m(t), V_m(t), \forall m, t\}$. The optimization problem is given as

$$\max_{\mathbf{U},\mathbf{P},\mathbf{G}} \quad \frac{R_{total}}{E_{total}} \quad (18a)$$

$$\text{s.t.} \quad q_m(1) = q_m(N), \forall m \quad (18b)$$

$$u_{m,i}(t) = \{0, 1\}, \forall m, i, t \quad (18c)$$

$$\sum_{m=1}^{2} u_{m,i}(t) \leq 1, \forall i, t \quad (18d)$$

$$\sum_{i=1}^{I} u_{m,i}(t) \leq 1, \forall m, t \quad (18e)$$

$$u_{m,i}(t) h_{m,i,1} \geq u_{m,i}(t) h_{m,i,2}, \forall i, m = 1 \quad (18f)$$

$$u_{m,i}(t) h_{m,i,1} \leq u_{m,i}(t) h_{m,i,2}, \forall i, m = 2 \quad (18g)$$

$$0 \leq P_{m,i}(t) \leq P_{\max}, \forall m, i \quad (18h)$$

$$P_{m,i,j}(t) \geq 0, \forall m, i, j \quad (18i)$$

$$q_m(t+1) = q_m(t) + V_m(t)\delta_t + \frac{1}{2} a_m(t) \delta_t^2, \forall m, t \quad (18j)$$

$$V_m(t+1) = V_m(t) + a_m(t)\delta_t, \forall m, t \quad (18k)$$

$$d_{\min}^2 \leq ||q_1(t) - q_2(t)||^2, \forall t \quad (18l)$$

$$V_{\min} \leq \parallel V_m(t) \parallel \leq V_{\max}, \forall m, t \quad (18m)$$

$$\parallel a_m(t) \parallel \leq a_{\max} \quad (18n)$$

$$r_{in} \leq d_{m,z}(t) \leq r_{out}, m = 1 \quad (18o)$$

$$d_{m,z}(t) \leq r_{in}, m = 2 \quad (18p)$$

$$u_{m,i}(t) R_{m,i,j}(t) \geq R_{\min}, \forall m, i, j, t \quad (18q)$$

where $P_{\max}$ denotes the maximum transmit power of UAV in one time slot, $R_{m,i,j}$ denotes the achievable rate of the node j in group i served by UAV m, $R_{\min}$ denotes the minimum communication rate threshold, $a_{\max}$ indicates the maximum acceleration of UAV, $V_{\max}$ and $V_{\min}$ represent the maximum and minimum velocity of UAV. (18f) and (18g) denote the relationship of channel power gain between UAVs and different nodes. (18m)-(18p) show the boundary constraints of the parameters. (18q) ensures the minimum communication rate of each node.

III. Solution Algorithm

Due to the objective function (18a) and constraints (18c), (18l), (18m), (18o), (18q) are non-convex, the mixed integer fraction optimization problem (18) is difficult to solve directly. Thus, we divide (18) into three sub-problems: communication scheduling optimization, UAV transmit power optimization and UAV motion parameters optimization. An effectively alternating iterative optimization algorithm is presented to solve (18).

A. Communication Scheduling Optimization

A NOMA grouping algorithm is proposed to pair the nodes in the inner circle with those in the annular region, which may improve NOMA performance by generating great distance difference for the nodes in one group. Then the sub-optimization problem for communication scheduling $\mathbf{U}$ is first considered with given UAV motion parameters $\mathbf{G}$ and UAV transmit power $\mathbf{P}$.

According to the distance from annular nodes to inner circle nodes, we pair the annular nodes with inner circle nodes furthest from it. If there is no duplicate pairing, the pairing is successful. Otherwise, keep the pairing of the farthest nodes, and the remaining annular nodes are paired with the second farthest inner circle nodes. Repeat this process until all nodes are paired. After a reasonable NOMA grouping, the sub-problem of $\mathbf{U}$ is given as

$$\max_{\mathbf{U}} \quad \frac{R_{total}}{E_{total}} \tag{19a}$$
$$\text{s.t.} \quad (18c) \sim (18g) \tag{19b}$$

which is a fractional programming problem. According to Generalized Fractional Programming Theory [34], we can transform its objective function into a linear form. A variable $\eta = \frac{R_{total}}{E_{total}}$ is introduced to convert the objective function $\frac{R_{total}}{E_{total}}$ into $R_{total} - \eta E_{total}$.

Due to that (19) is a discrete integer optimization problem that is difficult to solve, the binary variable $u_{m,i}(t)$ need to be relaxed into a continuous variable as follows

$$0 \le u_{m,i}(t) \le 1, \forall m, i, t \tag{20}$$

Hence, (19) is redescribed as

$$\max_{\mathbf{U}} \quad R_{total} - \eta E_{total} \tag{21a}$$
$$\text{s.t.} \quad 0 \le u_{m,i}(t) \le 1, \forall m, i, t \tag{21b}$$
$$\sum_{m=1}^{2} u_{m,i}(t) \le 1, \forall i, t \tag{21c}$$
$$\sum_{i=1}^{I} u_{m,i}(t) \le 1, \forall m, t \tag{21d}$$
$$u_{m,i}(t)h_{m,i,1} \ge u_{m,i}(t)h_{m,i,2}, \forall i, m = 1 \tag{21e}$$
$$u_{m,i}(t)h_{m,i,1} \le u_{m,i}(t)h_{m,i,2}, \forall i, m = 2 \tag{21f}$$

We can observe that (21) has been converted into a convex optimization problem, which can be solved directly with the optimization tool CVX. Then, we need to restore the $\mathbf{U}$ obtained by CVX to the initial binary variables. We set the maximum element of each row in $\mathbf{U}$ to 1 and the rest elements to 0, which is seen as the binary solutions of $\mathbf{U}$.

B. UAV Transmit Power Optimization

The second sub-problem of UAV transmit power $\mathbf{P}$ is considered with given communication scheduling $\mathbf{U}$ and UAV motion parameters $\mathbf{G}$. It is given as

$$\max_{\mathbf{P}} \quad R_{total} - \eta E_{total} \tag{22a}$$
$$\text{s.t.} \quad P_{m,i,j}(t) \ge 0, \forall m, i, j \tag{22b}$$
$$0 \le P_{m,i}(t) \le P_{\max}, \forall m, i \tag{22c}$$
$$u_{m,i}(t)R_{m,i,j}(t) \ge R_{\min}, \forall m, i, j, t \tag{22d}$$

Substituting (14) and (17), (22a) is rewritten as

$$(R_1 - \eta E_1) + (R_2 - \eta E_2) \tag{23}$$

Then (22) is divided into two sub-problems as

$$\max_{\mathbf{P_1}} \quad R_1 - \eta E_1 \tag{24a}$$
$$\text{s.t.} \quad (22b) \sim (22d) \tag{24b}$$

$$\max_{\mathbf{P_2}} \quad R_2 - \eta E_2 \tag{25a}$$
$$\text{s.t.} \quad (22b) \sim (22d) \tag{25b}$$

where $\mathbf{P_1} = \{P_{1,i}(t), \forall i, t\}$ and $\mathbf{P_2} = \{P_{2,i}(t), \forall i, t\}$ represent the transmit power allocations of UAV 1 and UAV 2, respectively.

The problems (24) and (25) satisfy the Slater's condition and can be solved by Lagrange multiplier method [35]. We introduce non-negative Lagrange multipliers λ_m, θ_m and $\omega_m, \forall m$ for constraints (22c) and (22d), respectively. Then, the Lagrange functions of (24) and (25) can be given by

$$\begin{aligned} L_m(\mathbf{P_m}, \lambda_m, \theta_m, \omega_m) &= Q_m(\mathbf{P_m}, \lambda_m, \theta_m, \omega_m) \\ &+ \sum_{t=1}^{N}\sum_{i=1}^{I} \theta_m u_{m,i}(t) \log_2\left(1 + \frac{P_{m,i,1}(t)h_{m,i,1}(t)}{\sigma^2}\right) \\ &+ \sum_{t=1}^{N}\sum_{i=1}^{I} \omega_m u_{m,i}(t) \log_2\left(1 + \frac{P_{m,i,2}(t)h_{m,i,2}(t)}{\sigma^2 + P_{m,i,1}(t)h_{m,i,2}(t)}\right), \\ & m = 1 \end{aligned} \tag{26}$$

$$\begin{aligned} L_m(\mathbf{P_m}, \lambda_m, \theta_m, \omega_m) &= Q_m(\mathbf{P_m}, \lambda_m, \theta_m, \omega_m) \\ &+ \sum_{t=1}^{N}\sum_{i=1}^{I} \theta_m u_{m,i}(t) \log_2\left(1 + \frac{P_{m,i,1}(t)h_{m,i,1}(t)}{\sigma^2 + P_{m,i,2}(t)h_{m,i,1}(t)}\right) \\ &+ \sum_{t=1}^{N}\sum_{i=1}^{I} \omega_m u_{m,i}(t) \log_2\left(1 + \frac{P_{m,i,2}(t)h_{m,i,2}(t)}{\sigma^2}\right), m = 2 \end{aligned} \tag{27}$$

where

$$\begin{aligned} Q_m(\mathbf{P_m}, \lambda_m, \theta_m, \omega_m) &= \sum_{t=1}^{N}\sum_{i=1}^{I} u_{m,i}(t)R_{m,i}(t) \\ &- \eta \sum_{t=1}^{N}\left(P_m^c(t) + \sum_{i=1}^{I} u_{m,i}(t)P_{m,i}(t)\right) + \sum_{t=1}^{N} \lambda_m P_{\max} \\ &- \sum_{t=1}^{N}\sum_{i=1}^{I} \lambda_m u_{m,i}(t)\Big(P_{m,i,1}(t) + P_{m,i,2}(t)\Big) \\ &- \sum_{t=1}^{N} \theta_m R_{\min} - \sum_{t=1}^{N} \omega_m R_{\min}, \forall m \end{aligned} \tag{28}$$

Furthermore, the dual functions of the two sub-problems can be denoted as

$$F_m(\lambda_m, \theta_m, \omega_m) = \max_{\mathbf{P_m}} L_m(\mathbf{P_m}, \lambda_m, \theta_m, \omega_m) \tag{29a}$$
$$\text{s.t.} \quad P_{m,i,j}(t) \ge 0, \forall m, i, j \tag{29b}$$

With the given Lagrange multipliers $\lambda_m, \theta_m, \omega_m$, problem (29) can be divided into $2NI$ parallel optimization problems

$$P^{\star}_{m,i,1}(t)=\left[\frac{\sigma^2(h_{m,i,1}(t)(1+\theta_m)-h_{m,i,2}(t)(1+\omega_m))}{h_{m,i,1}(t)h_{m,i,2}(t)(\omega_m-\theta_m)}\right]^{+},\forall i,t,\ m=1 \tag{33}$$

$$P^{\star}_{m,i,1}(t)=\left[\frac{1+\theta_m}{(\eta+\lambda_m)\ln 2}+\frac{\sigma^2(1+\theta_m)((h_{m,i,2}(t)-h_{m,i,1}(t))}{(\omega_m-\theta_m)h_{m,i,1}(t)h_{m,i,2}(t)}\right]^{+},\forall i,t,\ m=2 \tag{34}$$

$$P^{\star}_{m,i,2}(t)=\left[\frac{1+\omega_m}{(\eta+\lambda_m)\ln 2}+\frac{\sigma^2(1+\omega_m)((h_{m,i,2}(t)-h_{m,i,1}(t))}{(\omega_m-\theta_m)h_{m,i,1}(t)h_{m,i,2}(t)}\right]^{+},\forall i,t,\ m=1 \tag{35}$$

$$P^{\star}_{m,i,2}(t)=\left[\frac{\sigma^2(h_{m,i,1}(t)(1+\theta_m)-h_{m,i,2}(t)(1+\omega_m))}{h_{m,i,1}(t)h_{m,i,2}(t)(\omega_m-\theta_m)}\right]^{+},\forall i,t,\ m=2 \tag{36}$$

of $P_{m,i,1}(t)$ and $P_{m,i,2}(t)$. The parallel problems can be described as

$$\max_{\mathbf{P_m}}\ H_m(\mathbf{P_m}) \tag{30a}$$

$$\text{s.t.}\ \ P_{m,i,j}(t)\geq 0,\forall m,i,j \tag{30b}$$

where,

$$\begin{aligned}H_m(\mathbf{P_m})&=u_{m,i}(t)\log_2\left(1+\frac{P_{m,i,1}(t)\,h_{m,i,1}(t)}{\sigma^2}\right)\\&+u_{m,i}(t)\log_2\left(1+\frac{P_{m,i,2}(t)\,h_{m,i,2}(t)}{\sigma^2+P_{m,i,1}(t)h_{m,i,2}(t)}\right)\\&-u_{m,i}(t)\eta\Big(P_{m,i,1}(t)+P_{m,i,2}(t)\Big)\\&-\lambda_m u_{m,i}(t)\Big(P_{m,i,1}(t)+P_{m,i,2}(t)\Big)\\&+\theta_m u_{m,i}(t)\log_2\left(1+\frac{P_{m,i,1}(t)\,h_{m,i,1}(t)}{\sigma^2}\right)\\&+\omega_m u_{m,i}(t)\log_2\left(1+\frac{P_{m,i,2}(t)\,h_{m,i,2}(t)}{\sigma^2+P_{m,i,1}(t)h_{m,i,2}(t)}\right),m=1\end{aligned} \tag{31}$$

$$\begin{aligned}H_m(\mathbf{P_m})&=u_{m,i}(t)\log_2\left(1+\frac{P_{m,i,1}(t)\,h_{m,i,1}(t)}{\sigma^2+P_{m,i,2}(t)h_{m,i,1}(t)}\right)\\&+u_{m,i}(t)\log_2\left(1+\frac{P_{m,i,2}(t)\,h_{m,i,2}(t)}{\sigma^2}\right)\\&-u_{m,i}(t)\eta\Big(P_{m,i,1}(t)+P_{m,i,2}(t)\Big)\\&-\lambda_m u_{m,i}(t)\Big(P_{m,i,1}(t)+P_{m,i,2}(t)\Big)\\&+\theta_m u_{m,i}(t)\log_2\left(1+\frac{P_{m,i,1}(t)\,h_{m,i,1}(t)}{\sigma^2+P_{m,i,2}(t)h_{m,i,1}(t)}\right)\\&+\omega_m u_{m,i}(t)\log_2\left(1+\frac{P_{m,i,2}(t)\,h_{m,i,2}(t)}{\sigma^2}\right),m=2\end{aligned} \tag{32}$$

By making the partial derivatives of (31) and (32) in $P_{m,i,1}(t)$ and $P_{m,i,2}(t)$ equal to 0, respectively, we can obtain the closed-form solution of UAV transmit power, $P_{m,i,1}(t)$ and $P_{m,i,2}(t)$ for $m=1,2$, as (33) $\sim$ (36) at the top of this page, where $[A]^{+}=\max\{0,A\}$ is to guarantee that the power is not negative.

After obtaining the closed-form optimal solution of $\mathbf{P}^{\star}$, the subgradient descent method will be used to obtain the specific transmit power values by iteratively updating the Lagrange multipliers as

$$\lambda_m=\lambda_m-v_1\Delta\lambda_m,\forall m \tag{37}$$

$$\theta_m=\theta_m-v_2\Delta\theta_m,\forall m \tag{38}$$

$$\omega_m=\omega_m-v_3\Delta\mu_m,\forall m \tag{39}$$

where v_1, v_2 and v_3 denote the step lengths of each iteration, and $\Delta\lambda_m$, $\Delta\theta_m$, $\Delta\omega_m$ represent the subgradients of λ_m, θ_m, ω_m as

$$\Delta\lambda_m=NP_{\max}-\sum_{t=1}^{N}\sum_{i=1}^{I}u_{m,i}(t)P_{m,i}(t),\forall m \tag{40}$$

$$\Delta\theta_m=\sum_{t=1}^{N}\sum_{i=1}^{I}u_{m,i}(t)R_{m,i,1}(t)-NR_{\min},\forall m \tag{41}$$

$$\Delta\omega_m=\sum_{t=1}^{N}\sum_{i=1}^{I}u_{m,i}(t)R_{m,i,2}(t)-NR_{\min},\forall m \tag{42}$$

The iteration process terminates when λ_m, θ_m, ω_m are all convergent.

C. UAV Motion Parameters Optimization

The third sub-optimization problem for the UAV motion parameters $\mathbf{G}$ is considered with given communication scheduling $\mathbf{U}$ and UAV transmit power $\mathbf{P}$. It is described as

$$\max_{\mathbf{G}} \quad R_{total} - \eta E_{total} \tag{43a}$$

$$\text{s.t.} \quad q_m(t+1) = q_m(t) + V_m(t)\delta_t + \frac{1}{2}a_m(t)\delta_t^2, \forall m, t \tag{43b}$$

$$V_m(t+1) = V_m(t) + a_m(t)\delta_t, \forall m, t \tag{43c}$$

$$\parallel V_m(t) \parallel \leq V_{\max}, \forall m, t \tag{43d}$$

$$\parallel a_m(t) \parallel \leq a_{\max}, \forall m, t \tag{43e}$$

$$d_{m,z}(t) \leq r_{out}, m = 1 \tag{43f}$$

$$d_{m,z}(t) \leq r_{in}, m = 2 \tag{43g}$$

$$d_{\min}^2 \leq ||q_1(t) - q_2(t)||^2, \forall t \tag{43h}$$

$$r_{in} \leq d_{m,z}(t), m = 1 \tag{43i}$$

$$V_{\min} \leq \parallel V_m(t) \parallel, \forall m, t \tag{43j}$$

Due to that the objective function (43a) and constraints (43h) $\sim$ (43j) are all non-convex, (43) is hard to solve directly. By applying SCA method to tackle these constraints, we can solve (43) by CVX directly.

By substituting (7) into $R_{m,i}(t)$, we can get the throughput of UAV m with $d_{m,i,j}^2 = ||q_m(t) - q_{i,j}||^2$ as

$$R_{m,i}(t) = \log_2\left(1 + \frac{P_{m,i,1}(t)\beta_0}{\sigma^2 \parallel q_m(t) - q_{i,1}\parallel^2}\right) + \log_2\left(1 + \frac{P_{m,i,2}(t)\beta_0}{\sigma^2 \parallel q_m(t) - q_{i,2}\parallel^2 + \beta_0 P_{m,i,1}(t)}\right), m = 1 \tag{44}$$

$$R_{m,i}(t) = \log_2\left(1 + \frac{P_{m,i,1}(t)\beta_0}{\sigma^2 \parallel q_m(t) - q_{i,1}\parallel^2 + \beta_0 P_{m,i,2}(t)}\right) + \log_2\left(1 + \frac{P_{m,i,2}(t)\beta_0}{\sigma^2 \parallel q_m(t) - q_{i,2}\parallel^2}\right), m = 2 \tag{45}$$

Based on the SCA method, for any local points $||q_m^{(l)}(t) - q_{i,1}||^2$ and $||q_m^{(l)}(t) - q_{i,2}||^2$, the first-order Taylor expansion of $R_{m,i}(t)$ is used as the replaceable lower bound of $R_{m,i}(t)$, which is given as

$$R_{m,i}(t) \geq R_{m,i}^{lb}(t) = R_{m,i}^{(l)}(t) - \psi_{m,1}S_{m,1}^{(l)}(t) - \psi_{m,2}S_{m,2}^{(l)}(t), \forall m, i \tag{46}$$

where $\psi_{m,1}$ and $\psi_{m,2}$ for $m = 1, 2$ are given in (47) $\sim$ (50) at the top of next page, and $R_{m,i}^{(l)}(t)$, $S_{m,1}^{(l)}(t)$ and $S_{m,2}^{(l)}(t)$ are respectively given as

$$R_{m,i}^{(l)}(t) = \log_2\left(1 + \frac{\beta_0 P_{m,i,1}(t)}{\sigma^2 \parallel q_m^{(l)}(t) - q_{i,1}\parallel^2}\right) + \log_2\left(1 + \frac{\beta_0 P_{m,i,2}(t)}{\beta_0 P_{m,i,1}(t) + \sigma^2 \parallel q_m^{(l)}(t) - q_{i,2}\parallel^2}\right), m = 1 \tag{51}$$

$$R_{m,i}^{(l)}(t) = \log_2\left(1 + \frac{\beta_0 P_{m,i,1}(t)}{\beta_0 P_{m,i,2}(t) + \sigma^2 \parallel q_m^{(l)}(t) - q_{i,1}\parallel^2}\right) + \log_2\left(1 + \frac{\beta_0 P_{m,i,2}(t)}{\sigma^2 \parallel q_m^{(l)}(t) - q_{i,2}\parallel^2}\right), m = 2 \tag{52}$$

$$S_{m,1}^{(l)}(t) = \parallel q_m(t) - q_{i,1}\parallel^2 - \parallel q_m^{(l)}(t) - q_{i,1}\parallel^2, \forall m \tag{53}$$

$$S_{m,2}^{(l)}(t) = \parallel q_m(t) - q_{i,2}\parallel^2 - \parallel q_m^{(l)}(t) - q_{i,2}\parallel^2, \forall m \tag{54}$$

For boundary constraints (43h) $\sim$ (43j), we also use their first-order Taylor expansions to replace the original expressions, in order to convert non-convex constraints to convex constraints. Therefore, (43h) in l-th iteration can be converted to a convex constraint as

$$\begin{aligned} d_{\min}^2 \leq & \parallel q_1^{(l)}(t) - q_2^{(l)}(t)\parallel^2 \\ & + 2\left(q_1^{(l)}(t) - q_2^{(l)}(t)\right)^T\left(q_1(t) - q_2(t)\right) \\ & - 2\left(q_1^{(l)}(t) - q_2^{(l)}(t)\right)^T\left(q_1^{(l)}(t) - q_2^{(l)}(t)\right), \forall m \end{aligned} \tag{55}$$

Similarly, the constraint (43i) can be converted to

$$\begin{aligned} r_{in}^2 \leq & \left\|q_m^{(l)}(t) - Z(t)\right\|^2 \\ & + 2\left(q_m^{(l)}(t) - Z(t)\right)^T\left(q_m(t) - Z(t)\right) \\ & - 2\left(q_m^{(l)}(t) - Z(t)\right)^T\left(q_m^{(l)}(t) - Z(t)\right), \forall m \end{aligned} \tag{56}$$

where $Z(t) = (0, 0, H)$ denotes the z-axis coordinate of the UAV flight altitude.

Furthermore, to deal with the non-convex denominator of objective function and constraint (43j), we introduce a slack variable τ_m. Then E_m can be rewritten as

$$E_m^u = \sum_{t=1}^{N}\left(c_1 \parallel V_m(t)\parallel^3 + \frac{c_2}{\parallel \tau_m(t) \parallel}(1 + \frac{\parallel a_m(t)\parallel^2}{g^2}) + \sum_{i=1}^{I} u_{m,i}(t)P_{m,i}(t)\right), \forall m \tag{57}$$

In addition, the slack variable τ_m needs to be less than or equal to $\parallel V_m(t) \parallel$, and the optimal solution is obtained when $\tau_m = \parallel V_m(t) \parallel$. Hence, the inequality constraints can be described as

$$\parallel V_m(t) \parallel^2 \geq \tau_m^2 \tag{58}$$

$$\tau_m \geq V_{min} \tag{59}$$

It can be observed that (58) is still a non-convex constraint and can be converted into convex constraint by the SCA method. For any local point $V_m^{(l)}(t)$ in the l-th iteration, we have

$$\parallel V_m(t)\parallel^2 \geq V_m^{lb}(t) = \parallel V_m^{(l)}(t)\parallel^2 + 2V_m^{(l)}(t)^T\left(V_m(t) - V_m^{(l)}(t)\right) \tag{60}$$

$$\psi_{m,1}=\frac{\beta_0 P_{m,i,1}\left(t\right)}{\ln 2(\beta_0 P_{m,i,1}\left(t\right)+\sigma^2 \parallel q_m^{(l)}(t)-q_{i,1}\|^2) \parallel q_m^{(l)}(t)-q_{i,1}\|^2},\ m=1 \tag{47}$$

$$\psi_{m,1}=\frac{\sigma^2\beta_0 P_{m,i,1}\left(t\right)}{\ln 2((\sigma^2 \parallel q_m^{(l)}(t)-q_{i,1}\|^2+\beta_0 P_{m,i,2}\left(t\right))^2+\beta_0 P_{m,i,1}\left(t\right)(\beta_0 P_{m,i,2}\left(t\right)+\sigma^2 \parallel q_m^{(l)}(t)-q_{i,1}\|^2))},\ m=2 \tag{48}$$

$$\psi_{m,2}=\frac{\sigma^2\beta_0 P_{m,i,2}\left(t\right)}{\ln 2((\sigma^2 \parallel q_m^{(l)}(t)-q_{i,2}\|^2+\beta_0 P_{m,i,1}\left(t\right))^2+\beta_0 P_{m,i,2}\left(t\right)(\beta_0 P_{m,i,1}\left(t\right)+\sigma^2 \parallel q_m^{(l)}(t)-q_{i,2}\|^2))},\ m=1 \tag{49}$$

$$\psi_{m,2}=\frac{\beta_0 P_{m,i,2}\left(t\right)}{\ln 2(\beta_0 P_{m,i,2}\left(t\right)+\sigma^2 \parallel q_m^{(l)}(t)-q_{i,2}\|^2) \parallel q_m^{(l)}(t)-q_{i,2}\|^2},\ m=2 \tag{50}$$

Hence, the optimization problem of the UAV motion parameters $\mathbf{G}$ can be reformulated as

$$\max_{\mathbf{G}}\ R_{total}^{lb}-\eta E_{_{total}}^{u} \tag{61a}$$

$$\text{s.t.}\ \ V_m^{lb}(t)\geq\tau_m^2,\forall m \tag{61b}$$

$$(43b)\sim(43g),(55),(56),(59) \tag{61c}$$

where,

$$R_{total}^{lb}=\sum_{m=1}^{2}\sum_{n=1}^{N}\sum_{i=1}^{I}u_{m,i}(t)R_{m,i}^{lb}(t),\forall m \tag{62}$$

$$E_{total}^{u}=E_1^u+E_2^u \tag{63}$$

Obviously, the optimization problem (61) is convex and can be solved by CVX.

D. Joint Alternating Iterative Optimization

An alternating iterative optimization algorithm is proposed to solve the original problem (18) by alternatively optimizing communication scheduling $\mathbf{U}$, transmit power $\mathbf{P}$ and motion parameters $\mathbf{G}$ of UAVs, as shown in Algorithm 1. The optimal solutions to (18) can be obtained until the maximum number of iterations is reached or the target value converges.

Algorithm 1 Alternating iterative optimization.

Initialize: the maximum number of iterations l_{max}, the iteration index $l=1$, the UAV motion parameters $\mathbf{G}^{(l)}$, the UAV transmit power $\mathbf{P}^{(l)}$, and the UAV communication scheduling $\mathbf{U}^{(l)}$;

1: **repeat**
2: fixing $\mathbf{P}^{(l)}$ and $\mathbf{G}^{(l)}$, solve (21) to get solution $\mathbf{U}^{(l+1)}$;
3: fixing $\mathbf{U}^{(l)}$ and $\mathbf{G}^{(l)}$, solve (22) to get solution $\mathbf{P}^{(l+1)}$;
4: fixing $\mathbf{U}^{(l)}$ and $\mathbf{P}^{(l)}$, solve (61) to get solution $\mathbf{G}^{(l+1)}$;
5: set $l=l+1$;
6: **until** $l>l_{max}$ **or** target value converges;

Output: $\mathbf{U}$, $\mathbf{P}$, $\mathbf{G}$.

TABLE I: Simulation Parameters

Parameter	Value
number of nodes: K	20
number of groups: I	10
radius of cicular area: r_{out}	500m
radius of inner circle region: r_{in}	$250\sqrt{2}$m
channel power gain: β_0 [20]	-50dB
noise power: σ^2 [20]	-110dBm
length of one time slot: δ_t [19]	0.5s
UAV flight altitude: H [19]	100m
maximum speed of UAV: V_{max}	40m/s
minimum speed of UAV: V_{min}	3m/s
flight cycle time of the UAV: T	80s
maximum transmit power of UAV: P_{max} [19]	1W
propulsion power coefficient of UAV: $c1$ [20]	0.001
propulsion power coefficient of UAV: $c2$ [20]	2250
minimum communication rate threshold: $R_{\min}$	6bps/Hz

IV. Simulation Results

In this section, simulation results are given to verify and analyze the rationality of system model. Table I shows system parameter values in the simulations.

We take the center of the target area as the center of the initial circular trajectory of UAV. The trajectory radii of the two UAVs can be given by $r_1=\frac{r_{in}+r_{out}}{2}$ and $r_2=\frac{r_{in}}{2}$, respectively. Furthermore, we assume that the UAVs make a uniform circular motion in a initial state and the initial positions of two UAVs are 180 degrees apart. Hence, the initial velocity and trajectory of each UAV can be described as

$$V_m(t)=\left(\frac{2\pi r_m}{T}\cos\alpha_m,\frac{2\pi r_m}{T}\sin\alpha_m\right),\forall m \tag{64}$$

$$q_m(t)=\left(r_m\cos\alpha_m,r_m\sin\alpha_m\right),\forall m \tag{65}$$

where

$$\alpha_1=\frac{2\pi(n-1)}{N-1} \tag{66}$$

$$\alpha_2=\pi+\frac{2\pi(n-1)}{N-1} \tag{67}$$

Currently, there have been several studies on throughput and energy consumption optimization of UAV. To illustrate the advantages of maximizing energy efficiency, we use our system model to compare the performance of several optimization

schemes: the proposed energy efficiency (EE) maximization, energy minimization [17], and throughput maximization [18]. Figure 2 shows the convergence of algorithm 1 under different optimization goals. It can be seen that as the number of iterations increases, the results of the three schemes all converge. Among them, the energy efficiency of the EE-maximization scheme and the Energy-minimization scheme both show an upward trend, while the Throughput-maximization scheme has a downward trend. This is because the UAV needs to change its flight speed frequently, allowing itself to experience more time around the node for greater throughput. In the iterative process, the increase in throughput is smaller than the increase in propulsion energy consumption, which ultimately leads to a reduction in the energy efficiency of the system.

Figure 3 indicates initial and optimized trajectory of dual UAVs. The numbers next to the IoT nodes indicate different NOMA group indexes. It can be observed that the optimized trajectories are close to their respective near nodes, which will generate larger distance difference between the UAV and the nodes in one group and thus improve the transmission performance of NOMA group. Due to the flight area limitation, the optimized trajectory of UAV 1 is close to the boundary of the inner circle, which only slightly deviates from the boundary when it is close to the node 2 in the annular region. This may decrease the communication distance from UAV 1 to the nodes in the inner circle, thus improving the overall NOMA performance.

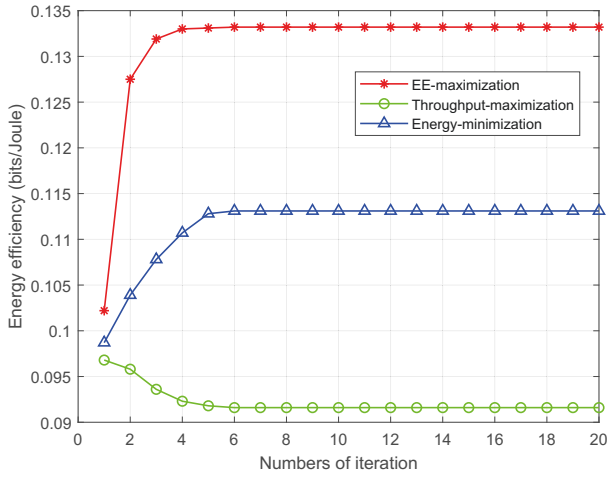

Fig. 2: Energy efficiency versus the number of iterations in different optimization schemes.

Figure 4 shows the UAV communication scheduling. We can see that the communication scheduling sequence is determined by the order of UAV flying over its nearby nodes. Figure 5 indicates the achievable rate of each node, where the red dotted line denotes the minimum communication rate required by each node. It is seen that all the nodes have satisfied the minimum communication rate requirement.

Figure 6 compares the energy efficiency of UAVs in different grouping scheme. In the random grouping scheme, we randomly pair adjacent nodes in inner circle and annular region. It indicates that the energy efficiency by random

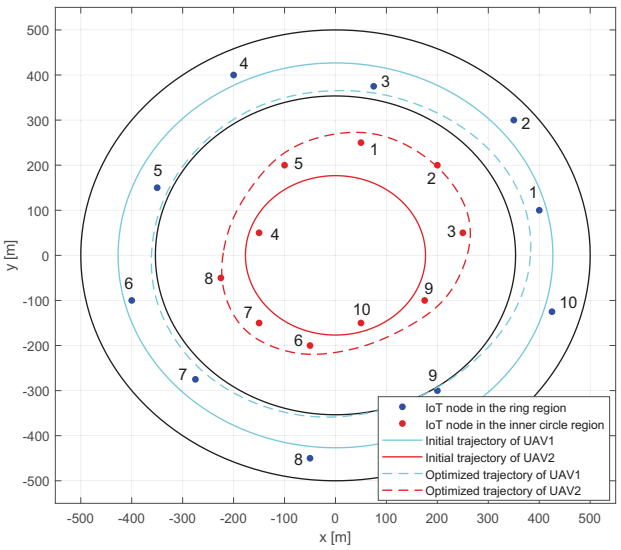

Fig. 3: Initial and optimized trajectories of dual UAVs.

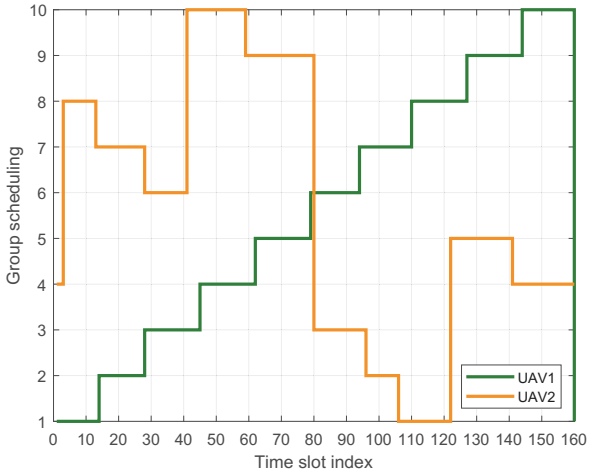

Fig. 4: UAV Communication scheduling.

grouping scheme is lower, which proves the superiority of our proposed grouping scheme. That is because the proposed NOMA grouping scheme can achieve greater distance difference for one group, which can improve NOMA decoding performance effectively.

Figure 7 shows UAV energy efficiency versus flight cycle time T in different optimization schemes. It indicates that in each optimization schemes, the energy efficiency decreases as T increases. This is because the transmit power limitation leads to a less improvement of UAV's throughput, but the propulsion power consumption will increase significantly. Therefore, the energy efficiency will decrease over the flight time.

Figure 8 compares energy efficiency with flight altitude under different optimization goals. It indicates that the sum energy efficiency decreases as the UAV's flight height increases. Because as the flight height increases, the distance

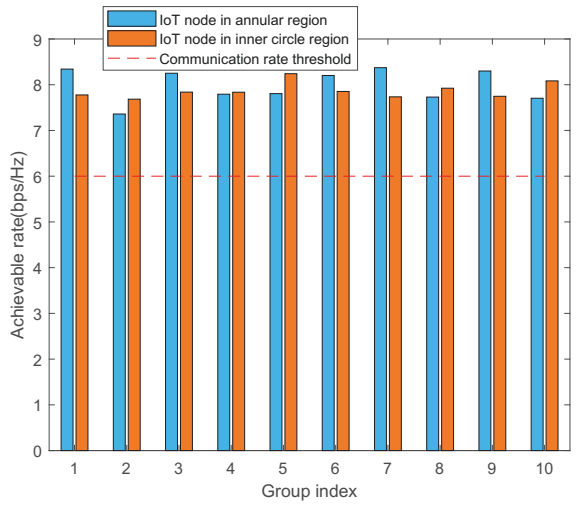

Fig. 5: Communication rates of IoT nodes.

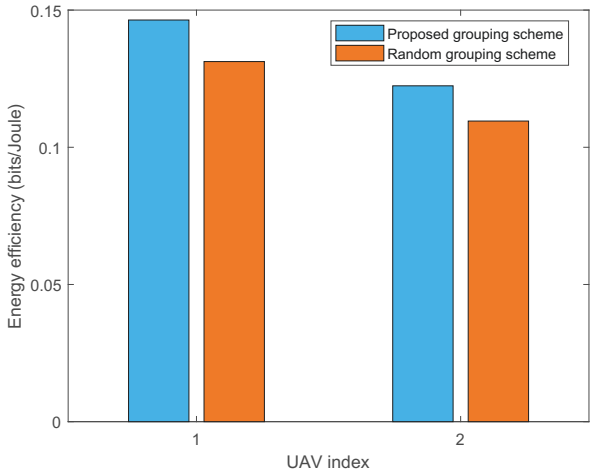

Fig. 6: Energy efficiency of UAVs in different grouping schemes.

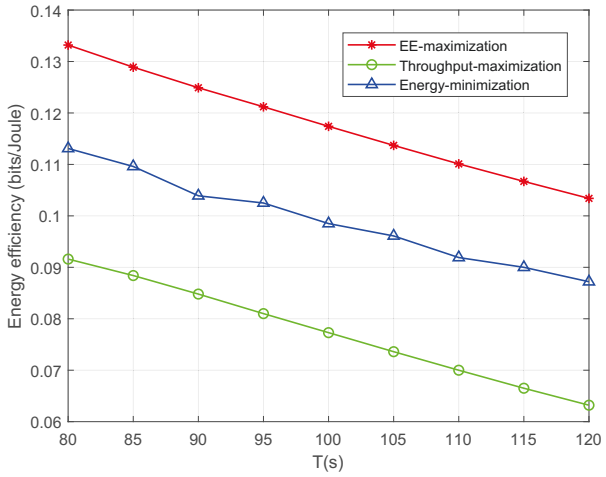

Fig. 7: Energy efficiency versus flight cycle time in different optimization schemes.

between the UAV and the node also increases, resulting in the sharp decrease of throughput under the limited transmit power of UAVs. Furthermore, the energy efficiency of Throughput-maximization scheme is lower than that of Energy-minimization scheme, but both the two schemes have lower energy efficiency than EE-maximization scheme. This result can be explained by Fig. 9.

Figure 9 shows the flight speeds of two UAVs with time slot under different optimization schemes. We can see that in the Throughput-maximization scheme, the UAV will consume more energy to frequently change its speed to fly towards the node for obtaining greater throughput, which results in the lowest energy efficiency in Fig. 8. In the EE-maximization scheme, the UAV speeds also change periodically to obtain greater throughput, but to decrease energy consumption, the UAV speeds change more gently than those in the throughput maximization scheme. In the Energy-minimization scheme, the UAV speeds will not change to keep lower energy consumption, which, however, leads to a smaller throughput for lower energy efficiency.

Figure 10 compares energy efficiency of the proposed varied UAV speed scheme with the traditional constant UAV speed scheme without kinematic constraints [32] and [33]. To verify the proposed system model, we also compare it with the system without the flight region constraints 1 and 2. We can observed that the energy efficiency of the varied speed scheme is significantly higher than that of the constant speed scheme. This is because in the varied speed scheme, the UAV can linger near the IoT node for a longer time by adjusting its flight speed, which can make the UAV obtain better channel gain to get larger throughput. In addition, we can see that the system performance will decrease when the flight region constraints are removed. This is because the distance difference from the UAV to the nodes in one group becomes smaller at this time, which will decrease the NOMA decoding performance.

Figure 11 compares energy efficiency versus UAV's transmit power in different optimization schemes. In the OMA-UAV mode, we use frequency division multiple access (FDMA) to divide the unit bandwidth into two parts for each node in one group. Then we get energy efficiency of OMA-UAV using optimized communication scheduling and UAV motion parameters. It is seen that the NOMA-UAV achieves higher energy efficiency than the OMA-UAV. Furthermore, it is seen that the NOMA-UAV under Throughput-maximization goal achieves lower energy efficiency than the OMA-UAV under the EE-maximization goal, which fully illustrates the huge impact of propulsion energy consumption on energy efficiency. In addition, We compare the energy efficiency between initial trajectory and optimized trajectory in the NOMA and OMA modes. It indicates that optimizing UAV motion parameters can significantly improve energy efficiency of UAVs.

V. Conclusions

In this paper, we propose a dual-NOMA-UAV assisted IoT, where two UAVs fly over the corresponding regions and serve the IoT nodes. The energy efficiency of UAVs is maximized by formulating a non-convex optimization problems under the

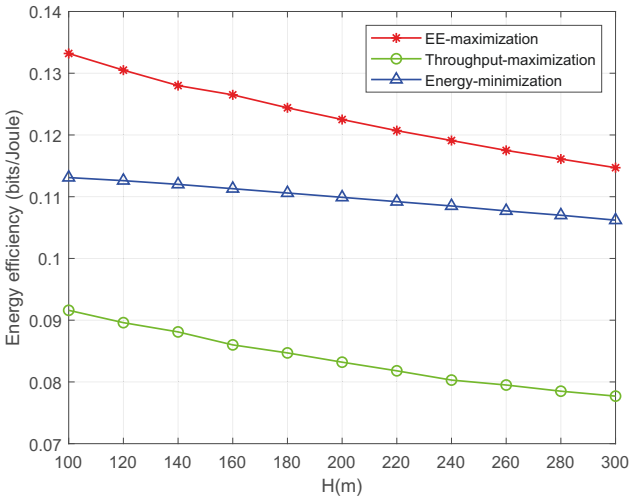

Fig. 8: Energy Efficiency versus flight altitude in different optimization schemes.

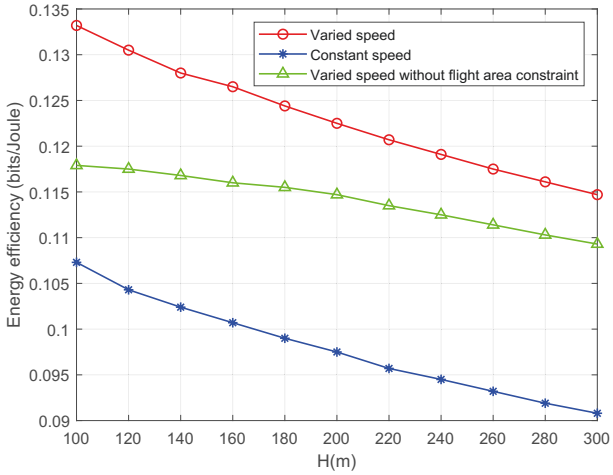

Fig. 10: Energy Efficiency versus flight altitude with different kinematic constraints.

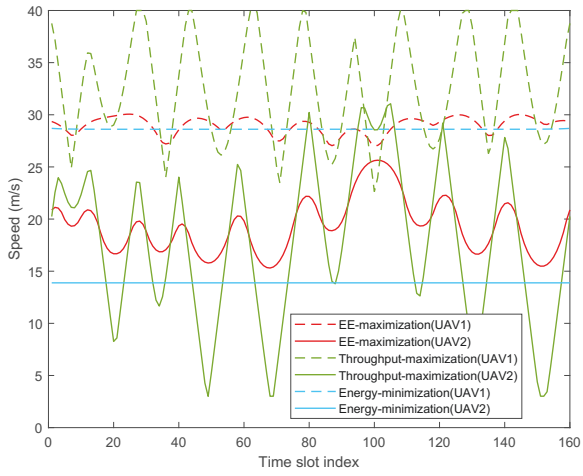

Fig. 9: UAV flight speed in different optimization schemes.

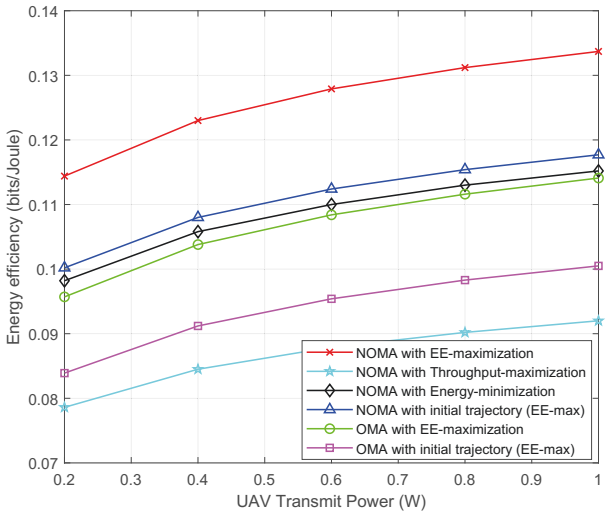

Fig. 11: Energy Efficiency versus transmit power in different optimization schemes.

varied UAV speeds and kinematic constraints. The non-convex optimization problem is divided into three sub-problems, each of which can be converted into convex optimization and solved by Lagrange multiplier method, sub-gradient descent method and SCA method. An alternating iterative optimization algorithm of the sub-problems is presented to solve the initial optimization problem. From the simulations, we can get the following conclusions. Firstly, energy efficiency maximization can decrease energy consumption and increase running time of UAVs while ensuring a certain throughput. Secondly, the flight period and flight trajectory will affect the energy efficiency of the UAVs, and optimizing UAV motion parameters can improve the energy efficiency effectively. Finally, compared with OMA-UAV, NOMA-UAV can achieve higher energy efficiency.

REFERENCES

[1] J. Leng, Z. Lin and P. Wang, "Poster Abstract: An Implementation of an Internet of Things System for Smart Hospitals," *2020 IEEE/ACM Fifth International Conference on Internet-of-Things Design and Implementation (IoTDI)* 2020, pp. 254-255.

[2] R. Yu, X. Zhang and M. Zhang, "Smart Home Security Analysis System Based on The Internet of Things," *2021 IEEE 2nd International Conference on Big Data, Artificial Intelligence and Internet of Things Engineeannular (ICBAIE)*, 2021, pp. 596-599.

[3] Y. Shaikh, V. K. Parvati and S. R. Biradar, "Survey of Smart Healthcare Systems using Internet of Things (IoT)," *2018 International Conference on Communication, Computing and Internet of Things (IC3IoT)*, 2018, pp. 508-513.

[4] C. Zhang, "Intelligent Internet of things service based on artificial intelligence technology," *2021 IEEE 2nd International Conference on Big Data, Artificial Intelligence and Internet of Things Engineeannular (ICBAIE)*, 2021, pp. 731-734.

[5] T. Guarda et al., "Internet of Things challenges," *2017 12th Iberian Conference on Information Systems and Technologies (CISTI)*, 2017, pp. 1-4.

[6] X. Liu, X. B. Zhai, W. Lu and C. Wu, "QoS-Guarantee Resource

Allocation for Multibeam Satellite Industrial Internet of Things With NOMA," *IEEE Transactions on Industrial Informatics*, vol. 17, no. 3, pp. 2052-2061, Mar. 2021.
[7] X. Liu, B. Lai, L. Gou, C. Lin and M. Zhou, "Joint Resource Optimization for UAV-Enabled Multichannel Internet of Things Based on Intelligent Fog Computing," *IEEE Transactions on Network Science and Engineeannular* , vol. 8, no. 4, pp. 2814-2824, Dec. 2021.
[8] O. M. Bushnaq, A. Chaaban and T. Y. Al-Naffouri, "The Role of UAV-IoT Networks in Future Wildfire Detection," *Internet of Things Journal*, vol. 8, no. 23, pp. 16984-16999, Dec, 2021.
[9] W. Feng, J. Wang, Y. Chen, X. Wang, N. Ge and J. Lu, "UAV-Aided MIMO Communications for 5G Internet of Things," *IEEE Internet of Things Journal*, vol. 6, no. 2, pp. 1731-1740, Apr. 2019.
[10] Z. Wang, R. Liu, Q. Liu, J. S. Thompson and M. Kadoch, "Energy-Efficient Data Collection and Device Positioning in UAV-Assisted IoT," *IEEE Internet of Things Journal*, vol. 7, no. 2, pp. 1122-1139, Feb. 2020.
[11] L. Gupta, R. Jain and G. Vaszkun, "Survey of Important Issues in UAV Communication Networks," *IEEE Communications Surveys and Tutorials*, vol. 18, no. 2, pp. 1123-1152, Secondquarter 2016.
[12] J. Gu, H. Wang, G. Ding, Y. Xu, Z. Xue and H. Zhou, "Energy-Constrained Completion Time Minimization in UAV-Enabled Internet of Things," *IEEE Internet of Things Journal*, vol. 7, no. 6, pp. 5491-5503, June, 2020.
[13] J. Wang, Z. Na and X. Liu, "Collaborative Design of Multi-UAV Trajectory and Resource Scheduling for 6G-Enabled Internet of Things,"*IEEE Internet of Things Journal*, vol. 8, no. 20, pp. 15096-15106, Oct, 2021.
[14] K. Li, W. Ni, E. Tovar and M. Guizani,"Joint Flight Cruise Control and Data Collection in UAV-Aided Internet of Things: An Onboard Deep Reinforcement Learning Approach" *IEEE Internet of Things Journal*, vol. 8, no. 12, pp. 9787-9799, June, 2021.
[15] B. Zhu, E. Bedeer, H. H. Nguyen, R. Barton and J. Henry, "Joint Cluster Head Selection and Trajectory Planning in UAV-Aided IoT Networks by Reinforcement Learning with Sequential Model," *IEEE Internet of Things Journal*, vol. 9, no. 14, pp. 12071-12084, July 2021.
[16] L. Yang, H. Yao, J. Wang, C. Jiang, A. Benslimane and Y. Liu, "Multi-UAV-Enabled Load-Balance Mobile-Edge Computing for IoT Networks," *IEEE Internet of Things Journal*, vol. 7, no. 8, pp. 6898-6908, Aug. 2020.
[17] Y. Zeng, J. Xu and R. Zhang, "Energy Minimization for Wireless Communication With Rotary-Wing UAV,"*IEEE Transactions on Wireless Communications*, vol. 18, no. 4, pp. 2329-2345, April 2019.
[18] Q. Wu and R. Zhang, "Common Throughput Maximization in UAV-Enabled OFDMA Systems With Delay Consideration" *IEEE Transactions on Communications*, vol. 66, no. 12, pp. 6614-6627, Dec. 2018.
[19] M. Hua, Y. Wang, Q. Wu, H. Dai, Y. Huang and L. Yang, "Energy-Efficient Cooperative Secure Transmission in Multi-UAV-Enabled Wireless Networks,"*IEEE Transactions on Vehicular Technology*, vol. 68, no. 8, pp. 7761-7775, Aug. 2019.
[20] Y. Zeng and R. Zhang, "Energy-Efficient UAV Communication With Trajectory Optimization," *IEEE Transactions on Wireless Communications*, vol. 16, no. 6, pp. 3747-3760, June, 2017.
[21] Q. Wu, Y. Zeng and R. Zhang, "Joint Trajectory and Communication Design for Multi-UAV Enabled Wireless Networks," *IEEE Transactions on Wireless Communications*, vol. 17, no. 3, pp. 2109-2121, Mar. 2018.
[22] Z. Li et al., "Energy Efficient Resource Allocation for UAV-Assisted Space-Air-Ground Internet of Remote Things Networks," *IEEE Access*, vol. 7, pp. 145348-145362, 2019.
[23] M. Katwe, K. Singh, P. K. Sharma, C. -P. Li and Z. Ding, "Dynamic User Clustering and Optimal Power Allocation in UAV-Assisted Full-Duplex Hybrid NOMA System," *IEEE Transactions on Wireless Communications*, vol. 21, no. 4, pp. 2573-2590, April 2022.
[24] B. Wang et al., "Graph-Based File Dispatching Protocol With D2D-Enhanced UAV-NOMA Communications in Large-Scale Networks," *IEEE Internet of Things Journal*, vol. 7, no. 9, pp. 8615-8630, Sept. 2020.
[25] X. Wu, Z. Wei, Z. Cheng and X. Zhang, "Joint optimization of UAV Trajectory and User Scheduling Based on NOMA Technology," *2020 IEEE Wireless Communications and Networking Conference (WCNC)*, 2020, pp. 1-6.
[26] D. Hu, Q. Zhang, Q. Li and J. Qin, "Joint Position, Decoding Order, and Power Allocation Optimization in UAV-Based NOMA Downlink Communications," *IEEE Systems Journal*, vol. 14, no. 2, pp. 2949-2960, June, 2020.
[27] Do et al., "UAV Relaying Enabled NOMA Network With Hybrid Duplexing and Multiple Antennas," *IEEE Access*, vol. 8, pp. 186993-187007, 2020.
[28] A. Masaracchia, L. D. Nguyen, T. Q. Duong, C. Yin, O. A. Dobre and E. Garcia-Palacios, "Energy-Efficient and Throughput Fair Resource Allocation for TS-NOMA UAV-Assisted Communications," *IEEE Transactions on Communications*, vol. 68, no. 11, pp. 7156-7169, Nov. 2020.
[29] M. Katwe, K. Singh, P. K. Sharma and C. -P. Li, "Energy Efficiency Maximization for UAV-Assisted Full-Duplex NOMA System: User Clustering and Resource Allocation," *IEEE Transactions on Green Communications and Networking*, vol. 6, no. 2, pp. 992-1008, June 2022.
[30] M. F. Sohail, C. Y. Leow and S. Won, "Energy-Efficient Non-Orthogonal Multiple Access for UAV Communication System," *IEEE Transactions on Vehicular Technology*, vol. 68, no. 11, pp. 10834-10845, Nov. 2019.
[31] H. Zhang, J. Zhang and K. Long, "Energy Efficiency Optimization for NOMA UAV Network With Imperfect CSI," *IEEE Journal on Selected Areas in Communications*, vol. 38, no. 12, pp. 2798-2809, Dec. 2020.
[32] Y. Li, H. Zhang, K. Long, C. Jiang and M. Guizani, "Joint Resource Allocation and Trajectory Optimization With QoS in UAV-Based NOMA Wireless Networks," *IEEE Transactions on Wireless Communications*, vol. 20, no. 10, pp. 6343-6355, Oct. 2021.
[33] X. Liu, Z. Liu and M. Zhou, "Fair Energy-Efficient Resource Optimization for Green Multi-NOMA-UAV assisted Internet of Things," *IEEE Transactions on Green Communications and Networking*, 2022, to appear.
[34] J. P. Crouzeix, J. A. Ferland and S. Schaible, "An Algorithm for Generalized Fractional Programs," *Journal of Optimization Theory and Applications*, vol.47, no.1, pp.35-49, Sep. 1985.
[35] S. Boyd and L. Vandenberghe, Convex Optimization. Cambridge, U.K.: Cambridge Univ. Press, 2004.

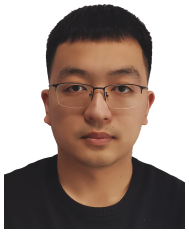

Zechen Liu received the B.S. degree from Shandong Agricultural University, China, in 2019. He is currently pursuing the Ph.D. degree with the School of Information and Communication Engineering, Dalian University of Technology, China. His current research interests focus on UAV-assisted wireless networks, integrated sensing and communications, and communication resource optimization.

Xin Liu (Senior Member, IEEE) received the M.Sc degree and the Ph.D. degree in Communication Engineering from the Harbin Institute of Technology in 2008 and 2012, respectively. He is currently an Associate Professor with the School of Information and Communication Engineering, Dalian University of Technology, China. From 2013 to 2016, he was a Lecturer with the College of Astronautics, Nanjing University of Aeronautics and Astronautics, China. His research interests focus on communication signal processing, cognitive radio, spectrum resource allocation, and broadband satellite communications.

Victor C. M. Leung (Life Fellow, IEEE) is a Distinguished Professor of Computer Science and Software Engineering at Shenzhen University, China. He is also an Emeritus Professor of Electrical and Computer Engineering and Director of the Laboratory for Wireless Networks and Mobile Systems at the University of British Columbia (UBC), Canada. His research is in the broad areas of wireless networks and mobile systems, and he has published widely in these areas. Dr. Leung is serving on the editorial boards of the IEEE Transactions on Green Communications and Networking, IEEE Transactions on Cloud Computing, IEEE Transactions on Computational Social Systems, IEEE Access, IEEE Network, and several other journals. He received the 1977 APEBC Gold Medal, 1977-1981 NSERC Postgraduate Scholarships, IEEE Vancouver Section Centennial Award, 2011 UBC Killam Research Prize, 2017 Canadian Award for Telecommunications Research, 2018 IEEE TCGCC Distinguished Technical Achievement Recognition Award, and 2018 ACM MSWiM Reginald Fessenden Award. He co-authored papers that won the 2017 IEEE ComSoc Fred W. Ellersick Prize, 2017 IEEE Systems Journal Best Paper Award, 2018 IEEE CSIM Best Journal Paper Award, and 2019 IEEE TCGCC Best Journal Paper Award. He is a Fellow of the Royal Society of Canada (Academy of Science), Canadian Academy of Engineering, and Engineering Institute of Canada. He is named in the current Clarivate Analytics list of Highly Cited Researchers.

Tariq S Durrani (Life Fellow, IEEE) is with the University of Strathclyde, Scotland, UK, where he was Deputy Principal of the University from 2000-06. After doctoral and postdoctoral research at Southampton, he joined the University of Strathclyde, Glasgow, as a Lecturer in 1976, and was appointed Professor of Signal Processing in 1982. He was Past Vice President of the IEEE and the Royal Society of Edinburgh, and Past President of the IEEE Signal Processing Society and of the IEEE Engineering Management Society. He is a Fellow of the Royal Academy of Engineering and the Royal Society of Edinburgh of UK, the National Academy of Engineering of USA, and the IEEE. His research interests include statistical signal and image processing, technology management, and higher education management.